Electronic Supplementary Material (ESI) for RSC Advances.

Supplementary Information

1. Curing of RMF resin

In order to investigate the curing behavior of the RMF resins, their mass loss during curing was determined. Prior to the measurement, five empty plastic cylinder molds were weighted. After the RMF sol was poured into five plastic cylinder molds, these cylinders were placed in an oven at 55°C for 24 hours while their weight was determined every hour on a KERN EWJ-300-3 balance. The RMF resins were then removed from the mold and dried in an oven at 55°C for 24 hours while their weight was determined every hour.

During the time the resins were in the mold, the weight loss was decreasing almost linearly (Fig. S1). After the resins were removed from the mold, the weight starts to decline rapidly. However, 33 hours after gelation, the weight remains constant.

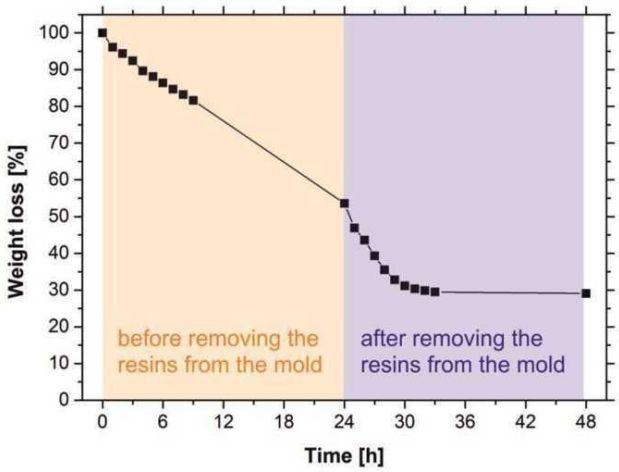

Fig. S1 Weight loss of the RMF resins during curing at 55°C

2. TGA-MS-IR

TGA measurements combined with mass spectroscopy and infrared spectroscopy (TGA-MS-IR) were conducted at on a NETZSCH TG 209 F1 Iris thermogravimetric analyzer with a heating rate of 5°C/min under Helium atmosphere with a flow rate of 50 ml/min. MS spectra were recorded by NETZSCH QMS 403C Aëolos and IR spectra on a Bruker Tensoer 27.

Fig. S2 illustrates the MS ion current curves of the (a) strong signals and the (b) weak signals. Between 50°C and 100°C a peak of the m/z=17 and m/z=18 ratio is observed which is attributed to the adsorbed moisture within the resin being released. Between 100°C and 300°C, m/z=35

and m/z=36 are attributed to the release of hydrochloric acid whereas m/z=85 might be explained by the release of piperidine. Above 300°C a second peak of m/z=17 and m/z=18 is an indication of the polycondensation reaction. The signal from m/z=44 is attributed to the release of CO_2 which indicates the oxidation of the carbon. Probably, the signal from m/z=30 does not originate from a single chemical compound. The first peak might come from the release of formaldehyde whereas the signals above 200°C might be attributed to the release of ethylamine which decomposes into $CH_2NH_2^{+\cdot}$.

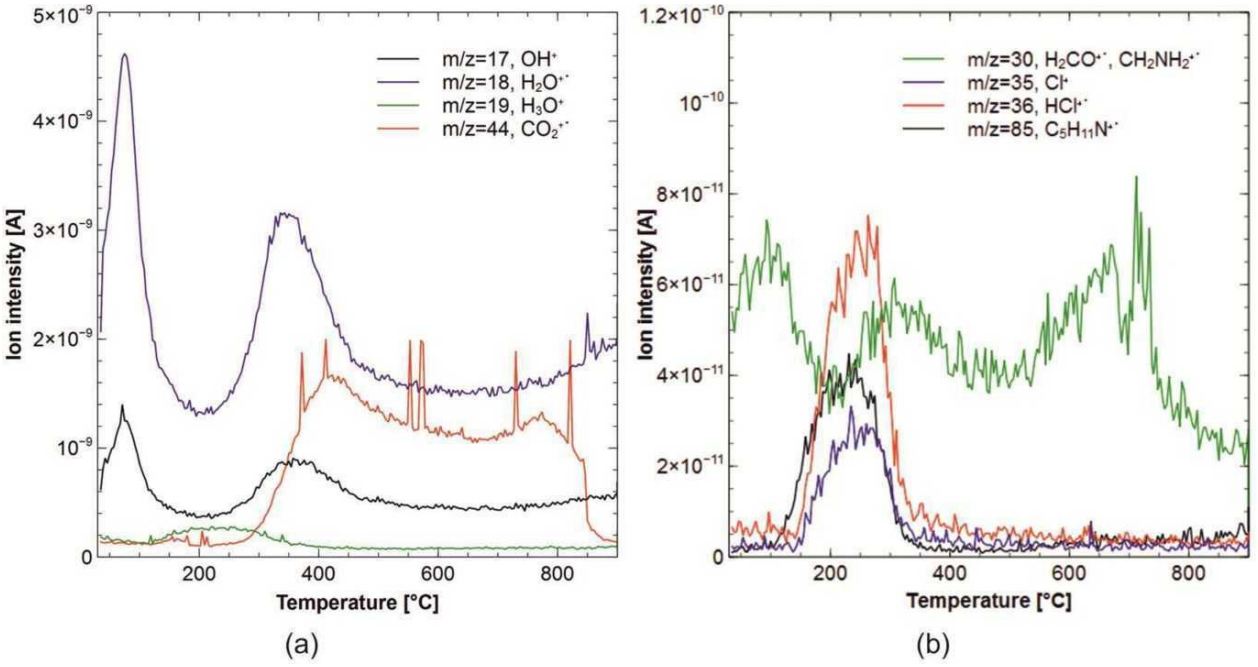

Fig. S2 MS analysis of gaseous products from sample A as a function of the pyrolysis temperature. Strong ion intensities are illustrated in (a) whereas weak signals are exhibited in (b).

The TGA-IR spectra exhibit the absorbance in dependence of the temperature and the wavenumber shown in Fig. S3. An intensive peak was detected at 2310 cm^{-1} which corresponds to the C=O stretching vibration. Between 350°C and 850°C the oxidation takes place as discussed above. At 250°C the vibration-rotation spectrum from HCl can be detected which is in agreement with the signal from TGA-MS. The signal at 3200 cm^{-1} and 3300 cm^{-1} comes from amine-containing groups and starts to increase above 350°C.

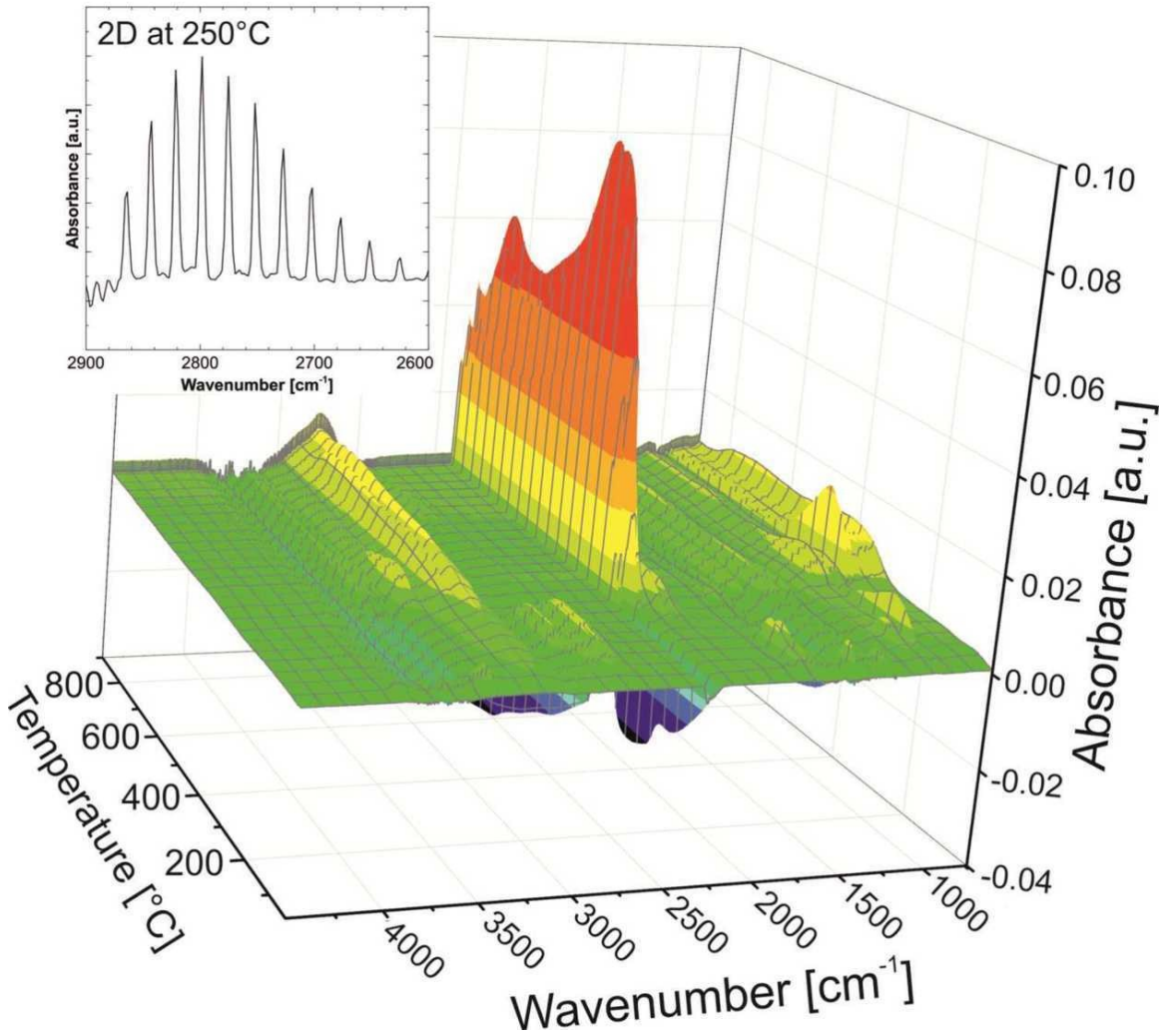

Fig. S3 3D representation of FTIR spectra of the volatile compounds of sample A

3. Raman spectroscopy

Samples were cut with a diamond saw into cylinders with a diameter of 10 mm and a height of 4 mm. After washing in acetone, the samples were dried in an oven at 50°C overnight.

The experimental procedure was the following: Raman spectra were measured on a Renishaw 2000 spectrometer equipped with holographic notch filters for elastic scattering and a CCD array detector. WiRE software was used to accumulate the data. The samples were excited with a HeNe laser (632.816 nm). The laser was focused onto the sample using a 20x objective. The instrument was calibrated with a Si single crystal (Raman band at ~520 cm^{-1}). The spectra were recorded at room temperature with an exposure time of 30 s and accumulation number of 5.

Raman spectra of RMF-derived carbons pyrolyzed at different temperatures are shown in Fig. S4. At approximately 1360 cm-1 and 1580 cm-1 two broad bands are present. At higher pyrolysis temperatures both, the D-band (1357 cm^{-1}, A_{1g}-mode) and the G-band (1580 cm^{-1}, E_{2g}-mode) start to broaden. Both bands are referred to sp^2-bonded carbon, while the D-band is specific for the ring-breathing mode of sp^2-bonded carbon in aromatic rings. Since the ring-breathing mode is enabled at defects and edge planes in graphite, the D-band is normally attributed to disorder.

The decrease in the intensity of the Raman-active bands with increasing pyrolysis temperature might indicate a higher degree of light absorption or reflection for the samples pyrolyzed at higher temperatures. However, the ratio of the D- and G-band intensities as well as the full width at half maximum of either band remains approximately constant upon pyrolysis in the investigated temperature range. Therefore, it can be concluded that there is no graphitization or pronounced improvement of ordering occurring for these samples, which is in agreement with the XRD results.

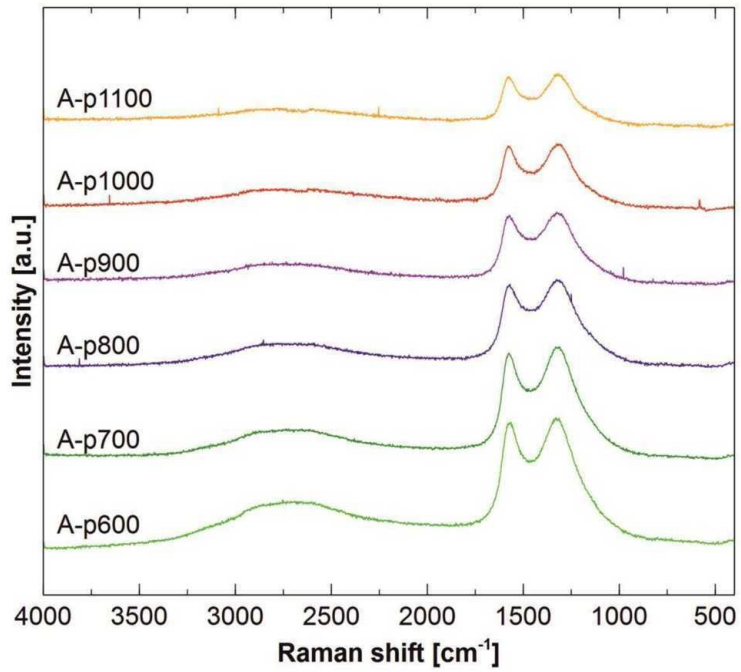

Fig. S4 Raman spectra of carbonized resins after different pyrolysis temperatures

4. XPS

The XPS results of the pyrolyzed and activated carbons are shown in Fig. S5 and Table S1. The N 1s spectra of carbons prepared at different pyrolysis temperatures has been considered to be a superposition of the signals of four different chemical states, namely pyridinic-type nitrogen (N-6), pyrrolic and/or pyridone-type nitrogen (N-5), quaternary nitrogen (N-Q) and pyridine nitrogen-oxide (N-X). These are the states that have been found in similar materials in literature [1,2]. Consequently the signal has been deconvoluted into four different peaks with the relative peak distances fixed according to the values reported by Pels *et al.* [1]. The FWHM was fixed to be ≤ 2.2 eV. The average value of the resulting peak positions were within ± 0.4 eV compared to the average reference values reported in literature [1,2]. This seems to be a reasonable accuracy and indicates that the fitting procedure and assumptions seem to be justified. Especially for the higher pyrolysis temperatures as well as the activated sample the signal to noise ratio is quite low. This means that e.g. for the KOH activated sample the observed pyrrolic/pyridone peak could be entirely due to the noise. In other words we do not expect a better accuracy than ± 3%. It can be observed that higher pyrolysis temperatures lead to a decrease of the pyrrolic and

pyridone-type nitrogen (N-5) concentration relative to the concentration of quaternary nitrogen (N-Q).

References

1 J. R. Pels, F. Kapteijn, J. a. Moulijn, Q. Zhu and K. M. Thomas, *Carbon N. Y.*, 1995, **33**, 1641–1653.

2 S. R. Kelemen, M. L. Gorbaty and P. J. Kwiatek, *Energy & Fuels*, 1994, **8**, 896–906.

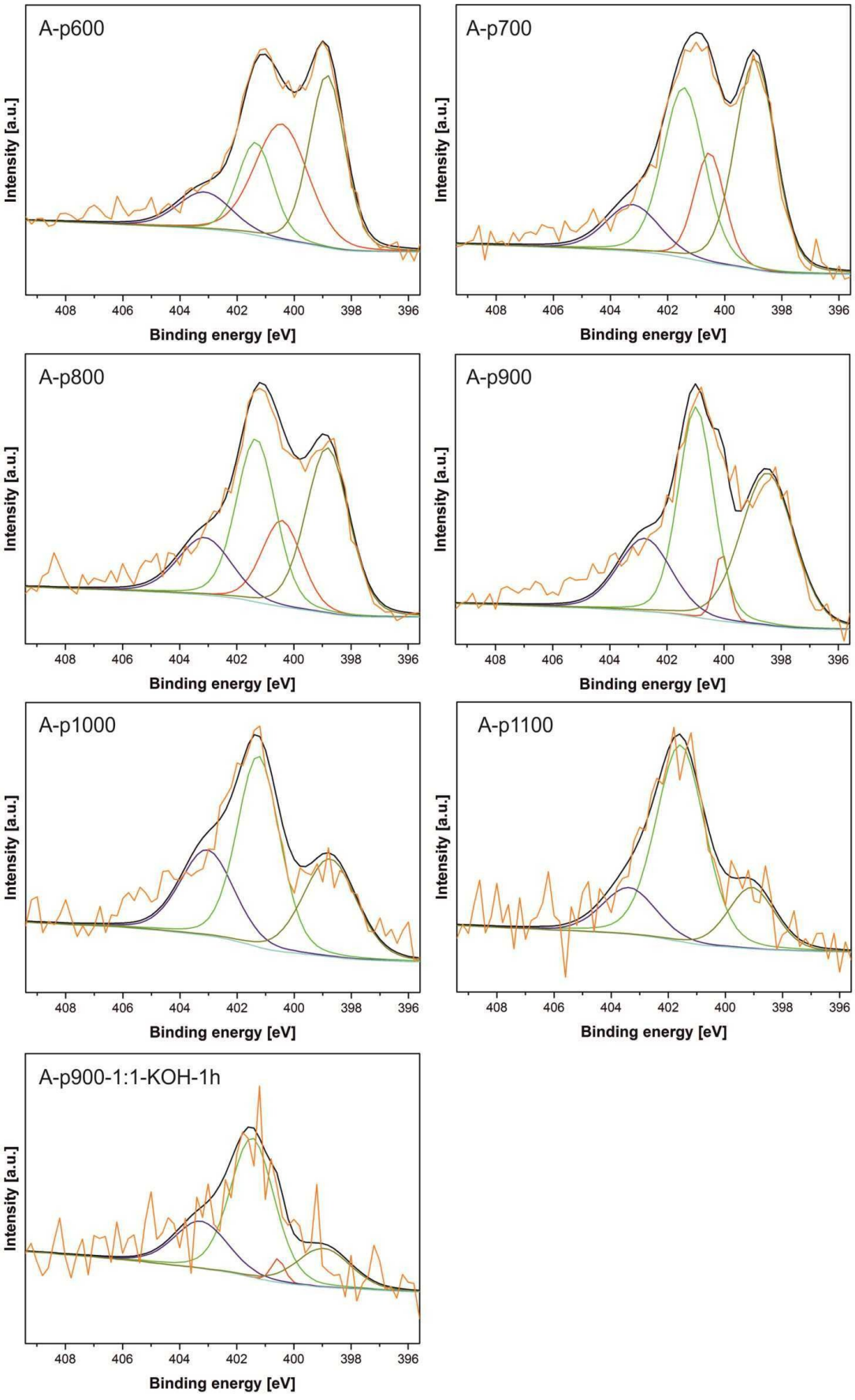
A-p600
A-p700
A-p800
A-p900
A-p1000
A-p1100
A-p900-1:1-KOH-1h
Intensity [a.u.]
Binding energy [eV]
408
406
404
402
400
398
396

Fig. S5 Deconvolution of the N 1s spectra of pyrolyzed and activated carbons

Table S1 Binding energies and relative surface concentration of nitrogen species obtained by fitting the N 1s core level XPS spectra (* represents sample A-p900-1:1-KOH-1h)

Sample	N-6			N-5			N-Q			N-X		
	B.E. [eV]	FWHM	%	B.E. [eV]	FWHM	%	B.E. [eV]	FWHM	%	B.E. [eV]	FWHM	%
A-p600	398.85	1.46	34.86	400.45	2.2	35.24	401.35	1.45	18.65	403.15	2.2	11.26
A-p700	398.93	1.66	39.47	400.53	1.25	16.18	401.43	1.73	32.39	403.23	2.2	11.96
A-p800	398.82	1.78	35.56	400.42	1.64	17.10	401.32	1.63	32.07	403.12	2.2	15.27
A-p900	398.48	2.2	39.85	400.08	0.59	4.86	400.98	1.45	36.22	402.78	2.2	19.07
A-p1000	398.75	2.2	29.10	-	-	0.00	401.25	1.76	45.37	403.05	2.2	25.52
A-p1100	399.07	1.92	19.17	-	-	0.00	401.57	2.02	64.21	403.37	2.2	16.62
A-KOH*	398.95	2.18	18.60	400.55	0.55	2.90	401.45	1.82	55.63	403.25	2.2	22.87